Annals of R.S.C.B., ISSN:1583-6258, Vol. 25, Issue 4, 2021, Pages. 618 - 639
Received 05 March 2021; Accepted 01 April 2021.

Design and Simulation of MEMS Piezoelectric Cantilever Array for Fully Cochlear Implantable Sensor

Abdul Aziz Khan J [1], Shanmugaraja P [2],Kannan S [3]

[1]Research Scholar, Department of Electronics and Communication Engineering, Annamalai University,Chidambaram, Annamalai Nagar 608002, India
[2]Professor, Department of Electronics and Instrumentation Engineering, Annamalai University, Chidambaram, Annamalai Nagar 608002, India
[3]Research Scholar, Department of Electronics and Instrumentation Engineering, Annamalai University, Chidambaram, Annamalai Nagar 608002, India
jahanaziz858@gmail.com[1],psraja70@gmail.com[2],kannan.blitz@gmail.com[3]

Abstract---This paper presents the improving area-efficient MEMS (Micro-Electrical Mechanical System) piezoelectric cantilever array prototype for a fully cochlear implantable sensor. The proposed design consists of seventeen cantilevers in an array arrangement connected in parallel; the acoustic sound pressure level input considered to lies in between 60 and 94 dB SPL. Deflection of the beam is measured in the frequency range from 300 Hz to 3700 kHz and the prototype can be fixed in the ear-drum. The acoustic SPL level matches and resonates with the frequency of the cantilever beam which stimulates the auditory nerve via cochlea and sends the information to the brain. As a result, the proposed device shows the maximum electric potential voltage, displacement, and von Mises stress as obtained using simulation. This method makes viability to reduce environmental noise with a precision level of hearing and makes more comfort to the future generation for a deaf-mute person. The main aim of this proposed system is to provide an improving area-efficient MEMS (Micro-Electrical Mechanical System) piezoelectric cantilever array to obtain maximum electric potential voltage for a fully cochlear implantable sensor is focused in this work.

Keywords---Micro-Electrical Mechanical System (MEMS), Piezoelectric cantilever, Fully cochlear implantable sensor.

1. Introduction

As stated by WHO in one of its surveys, over 5% of the world population, 466 million individuals have hearing losses, particularly 432 million grownups, and 34 million youngsters, and it is assessed 900 million individuals will have hearing misfortunes by the time of 2050 [1]. The ear plays a vital role in hearing and maintaining balance and hence it receives sound and converts it into electrical signals, causes nerve impulses to be sent to the brain. The human hearing frequency range varies from 20Hz to 200kHz, although human speech frequency extends from 250Hz to 4kHz loudness and pitch can be high or low depending on the speech. It is very crucial to understand the speech in between 4 to 8kHz, exceptionally during noise nuisance and confusing activity, the frequency range varies above 100dB sound pressure level it makes more discomfort [2,3]. Hearing loss can be classified into three types: sensorineural, conductive, and mixed hearing loss [4]. In the sensorineural loss, inner ear nerves and hair cells are harmed may be owing to aging, drug toxicity, sickness, or noise damage [5]. In Conductive loss, sounds that cannot pass through the outer and middle ear may be owing to fluid, ear infection, tumors, hole in the eardrum, stuck in-ear canal [6]. A mixed blend of sensorineural and conductive hearing loss might make hearing worse [7]. There are three parts of the ear to detect the sound: outer, middle, and inner. The outer ear assembles sound from the auricle through the external acoustic meatus (Ear canal) and arrives at the tympanic membrane (Eardrum). The middle ear has a tympanic membrane, tympanic cavity, and ossicles (the three tiny bones: Malleus, incus, and stapes). The vibrations on tiny bones are transformed into the cochlea. The inner ear has an oval window, semicircular ducts and cochlea. The semicircular ducts are loaded up with fluid and attached to the cochlea and nerves. It sends instructions on balance and head posture to the brain [8].

The Majority of the hearing losses can be treated by Conventional hearing aids, Middle ear implants (MEIs) or, cochlear implants (CIs). The Conventional hearing aid gets the sound, intensifies (amplifies), and changes over into electrical signals through a Vibro-acoustic speaker and sends to the brain (this utilizes receiver, amplifier, battery, volume control, and program button) [9]. The different styles of conventional hearing aid devices like BTE, ITE, ITC can be placed behind, in the ear and canal. Three aids are examined by leading manufacturers and tested with a huge number of patients. The environmental noise due to circumstances, discomfort, radiation noise in different situations while wearing the device [10]. In Middle ear implants (MEIs) or Cochlear implants (CIs) sound gets into the microphone. The processor picks sound from the microphone and sends it to the stimulator which is placed under the skin. The sound signals are converted to electric impulses by the stimulator. The electrode array collects the signals from the stimulator through the cochlea and passes to the brain [11]. CIs have some limitations such as time constraints, surgical risk, high cost, injury to the nerve [12].The MEMS-based implantable sensor is introduced and widely used to reduce size of the device, low cost, and power consumption. The main parameters to be focused on this sensor are frequency range, EIN SPL, dimension, power consumption and electric potential voltage. The first MEMS implantable sensor was the piezoresistive MEMS sensor proposed by Park et al. with a wide frequency range, reduced dimension, low power consumption nevertheless the high level of surgical issues, supporting ends are needed. MEMS capacitive displacement sensor proposed by ko et al. and Sache et al. on the other hand, MEMS capacitive accelerometer sensor proposed by Zurcher et al. resulted in a large frequency range above SPL nevertheless large power consumption [13]. The authors Yip et al. and Berker et al. focusing on materials of MEMS Piezoelectric force transducer and accelerometer sensor to reduce the power consumption by different methods [14]. The main intents while designing a fully cochlear implantable sensor are self-powered, reduced in size(micro-level), less noise, precision on hearing frequencies, self-analyzing, bandwidth, dynamic range.

In the existing device, eight cantilever beams were designed with a thin film piezoelectric acoustic transducer with sound pressure level input as 110 dB for electric potential voltage output of 114 mV to 140 mv were simulated for cochlear implant applications [15]. This paper proposes the improved area-efficient MEMS piezoelectric cantilever array (PCA)for a fully cochlear implant to overcome the limitations and barriers from existing cochlear implants (CIs). The MEMS PCA is placed on the eardrum, and the design is made up of seventeen thin piezoelectric cantilever beams which are connected in parallel to make it efficient within the size of the device. Each beam responds to the particular human speech frequency within the available bandwidth, the sensor reference input is given at a sound pressure level of 1 Pa (94dB) to produce electric potential voltage output of 135 mV. Parameters such as electric potential voltage, von Mises stress, displacement are obtained for all seventeen MEMS piezoelectric

Annals of R.S.C.B., ISSN:1583-6258, Vol. 25, Issue 4, 2021, Pages. 618 - 639
Received 05 March 2021; Accepted 01 April 2021.

cantilever beams [16]. The results have been discussed and analyzed by using COMSOL Multiphysics.

2. Design of PZT Cantilever Array

Fig 1. shows a schematic of the complete design of the proposed system. The main challenges while designing the proposed system are to reduce the area and to design more cantilever beams connected parallel within the area of 4.3×2.4mm. Piezoelectric Cantilever Array(PCA) consists of seventeen cantilever beams that resonate at a particular frequency in cochlea within the hearing bandwidth of 250Hz to 4kHz, the acoustic sound pressure level of 60 to 94 dB. Sound enters into the eardrum where the cantilever array is fixed, starts to vibrate the beam which is designed to that particular frequency, and resonates the particular frequency band in the cochlea [17]. The electric potential voltage(mV/Pa) for the particular beam is generated and the information passes through the auditory nerve via cochlea to the brain as shown in fig.1. The size of the device is reduced (4.3×2.4mm) and more cantilever beams to obtain the maximum electric potential voltage, Von misses stress, and displacement are simulated. The maximum electric potential voltage (mV/Pa) is produced for the input sound pressure level (SPL) of 94 dB (one Pascal) [18].

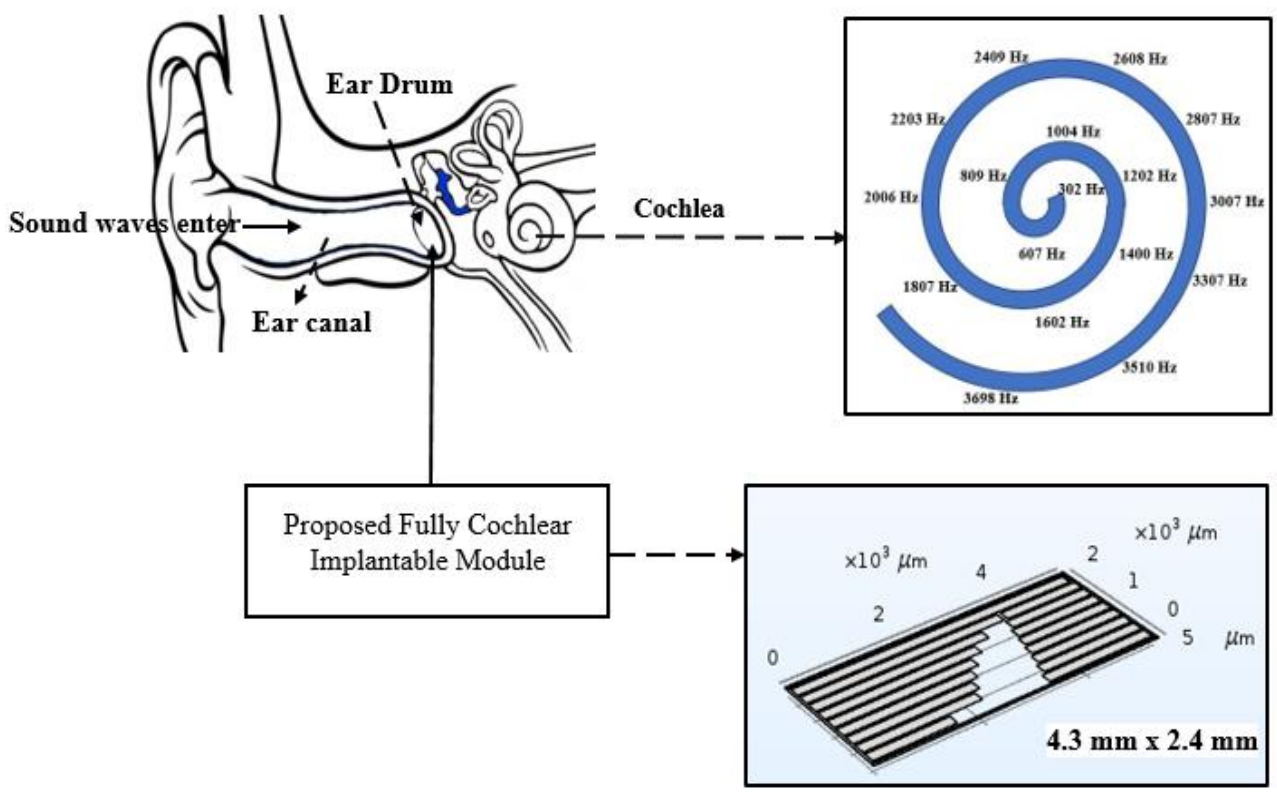

Figure 1. Schematic structure of proposed system

Annals of R.S.C.B., ISSN:1583-6258, Vol. 25, Issue 4, 2021, Pages. 618 - 639
Received 05 March 2021; Accepted 01 April 2021.

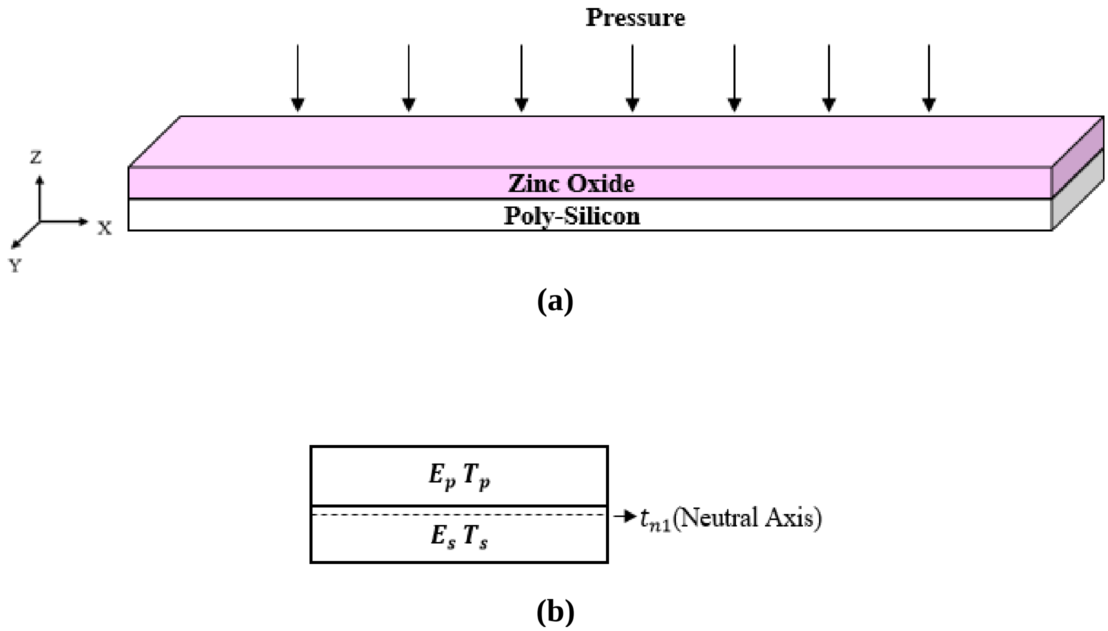

Figure 2. (a) Schematic view of Piezoelectric Cantilever beam (b) Cross-sectional view of Cantilever

Zinc Oxide(ZnO) is chosen as the uppermost layer and doped polysilicon is used as the substrate. The proposed MEMS piezoelectric cantilever beam is shown in Fig.2 consisting of a piezoelectric layer bonded with the Poly-silicon. The two materials are bonded perfectly along the X, Y, and Z axes [19]. One end of the cantilever beam is fixed at X=0 another end is kept free to deflect on the Z-axis. The width and thickness of the beam are kept constant (500 µm, 5200 µm) for all cantilever designs which deflects on its two layers on the Y-axis and Z-axis. The thickness of polysilicon and ZnO is defined as t_s and t_p.The neutral axis t_{n1} is based on the young's modulus and thickness of Poly-silicon and ZnO layers respectively. Considering the pressure P is applied in a direction perpendicular to the cantilever beam as shown in Fig 2(a). Beams of different lengths are simulated for Eigen frequencies from 300 to 3700 Hz, the width and thickness of the beam are kept constant and the frequency versus length plot is shown in Fig 3.

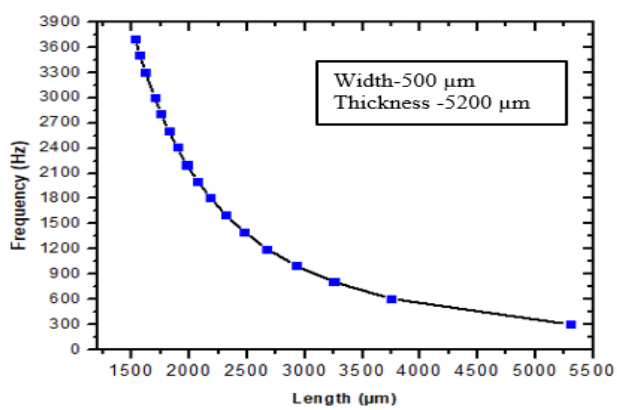

Figure 3. Frequency Vs Length of Piezoelectric Cantilever beams.

Annals of R.S.C.B., ISSN:1583-6258, Vol. 25, Issue 4, 2021, Pages. 618 - 639
Received 05 March 2021; Accepted 01 April 2021.

In this model, Zinc Oxide(ZnO) is suitable when compared to other materials because its piezoelectric coefficients and coefficient of electromechanical transformation of ZnO are relatively high. This makes ZnO an excellent material to be used widely in MEMS piezoelectric applications. It is also used in mobile communication, optoelectronics, and thin-film resonators for bulk acoustic waves.

Table 1. Piezoelectric coefficients for Zinc Oxide.

Parameters	Value
Piezoelectric coefficients (Strain)	d31=5.10-12 C/N d33=12,4.10-12 C/N
Piezoelectric coefficients (Voltage)	g31=0,36 Vm/N g33=1,57 Vm/N
Coefficient of electromechanical transformation	k=0,33
Elasticity modulus	Y=30-200 GPa
Relative dielectric permittivity	εr=10-11

3. Modeling and Fabrication

3.1 Displacement modelling

Pressure is applied as boundary load in the z-axis direction, the displacement of the Z-axis component of the beam induces electric potential voltage thereby stress or strain is produced. The inverse of the radius of curvature(r) can be expressed as shown in the below equation 1.

$$\frac{1}{r} = \frac{d^2h(x)}{dx^2} = \frac{M(x)}{WD_1} = -\frac{F}{WD_1}[L - x] \qquad (1)$$

The x values varies from 0< x<L, where $h(x)$=Axial Displacement ,$M(x)$=Bending moment of the cantilever, D_1=Bending Modulus per unit width can be expressed as equation 2.

$$D_1 = \frac{E_s^2 t_s^4 + E_p^2 t_p^4 + 2E_s E_p t_s t_p + (2t_s^2 + 2t_p^2 + 3t_s t_p)}{12(E_s t_s + E_p t_p)} \qquad (2)$$

where, E_s and E_p are the Young's Modulus of polysilicon and piezoelectric layers. The parameters$t_s$and t_p are the thickness of the polysilicon substrate and piezoelectric layer [20]. Equation 3 shows the boundary condition which is followed to solve the axial and tip displacement of the cantilever beam, initially the axial displacement to be derived is kept at zero on its fixed end. It can be written as

$$h_{(x=0)} = 0 \; and \; \left.\frac{dh}{dx}\right|_{x=0} = 0 \qquad (3)$$

By applying boundary condition, the equation (1) is solved and axial displacement is obtained

Annals of R.S.C.B., ISSN:1583-6258, Vol. 25, Issue 4, 2021, Pages. 618 - 639
Received 05 March 2021; Accepted 01 April 2021.

$$\frac{dh}{dx} = -\int \frac{F}{2WD_1}[L-x]^2 d \qquad (4)$$

$$\frac{dh}{dx} = -\frac{F}{2WD_1}\left[L^2 x - 2L\frac{x^2}{2} + \frac{x^3}{3}\right] + K_1 \quad (5)$$

$$h = -\frac{F}{2WD_1}\left[L^2 \frac{x^2}{2} - L\frac{x^3}{3} + \frac{x^4}{12}\right] + K_2 \qquad (6)$$

$$h_{tip} = -\frac{F}{WD_1}\left[\frac{L^4}{8}\right] \qquad (7)$$

In equation 8, W & L are width and length of the polysilicon substrate and Force F in terms of pressure P is applied in Pascal (Pa). Stiffness constant(k) of the beam is defined as the force required for unit tip displacement can be derived from equation (8).

$$k=\frac{\boldsymbol{Fa}}{\boldsymbol{h_{tip}}} = \frac{\boldsymbol{8WD_1}}{\boldsymbol{L^3}} \qquad (8)$$

3.2 Frequency Response

The resonant frequency 300Hz to 3700Hz is calculated manually by equation 10,11 and compared with the simulated frequency studies using COMSOL Multiphysics.

$$S_{d1} = \frac{2}{3}\frac{Wt_{seq}e_{31}}{W_n^2} \qquad (9)$$

$$K = \frac{8WD_1}{L^3} \text{ and } W_n = \sqrt{\frac{K}{M}} \qquad (10)$$

$$F = \frac{1}{2\pi}\sqrt{\frac{K}{M}} \qquad (11)$$

3.3 Stress and Displacement Analysis

The length of the beam(L) varies from 1528µm to 5300µm, the width(W) and the thickness($\boldsymbol{t_s}$&$\boldsymbol{t_p}$)are kept constant at 200µm, 5µm for the desired frequencies and simulated by COMSOL Multiphysics. The thickness of the ZnO is selected to induce maximum stress s that maximum electric potential is obtained. The Piezoelectric material ZnO is coated on the polysilicon substrate on the neutral axis.

$$\boldsymbol{t_s} = \sqrt{\frac{\boldsymbol{E_p}}{\boldsymbol{E_s}}}\boldsymbol{t_p} \qquad (12)$$

3.4 Material Properties

ZnO is selected as piezoelectric material and its standard elasticity matrix(C_E), the relative permittivity matrix(ε_{rs}) are used in COMSOL Multiphysics.

Annals of R.S.C.B., ISSN:1583-6258, Vol. 25, Issue 4, 2021, Pages. 618 - 639
Received 05 March 2021; Accepted 01 April 2021.

$$C_E = \begin{bmatrix} 209 & 121.1 & 105 & 0 & 0 & 0 \\ 0 & 209 & 105 & 0 & 0 & 0 \\ 0 & 0 & 211 & 0 & 0 & 0 \\ 0 & 0 & 0 & 42.3 & 0 & 0 \\ 0 & 0 & 0 & 0 & 42.3 & 0 \\ 0 & 0 & 0 & 0 & 0 & 44.2 \end{bmatrix} [GPa]$$

$$e_{ES} = \begin{bmatrix} 0 & 0 & -0.567 \\ 0 & 0 & -0.567 \\ 0 & 0 & 1.032 \\ 0 & 0 & 0 \\ 0 & -0.480 & 0 \\ -0.480 & 0 & 0 \end{bmatrix} [C/m^2]$$

$$\varepsilon_{rs} = \begin{bmatrix} 8.546 & 0 & 0 \\ 0 & 8.546 & 0 \\ 0 & 0 & 10.204 \end{bmatrix} [F/m]$$

Table 2. Physical Properties of the materials

Materials	Young's Modulus (GPa)	Poison's Ratio	Density (kg/m^3)
Poly-Si	160	0.22	2320
ZnO	161	0.35	5680

With the equation 10and 11, we have obtained and verified the Eigen frequency with the manual modeling. The calculated frequency, voltage vs simulated frequency, voltage is verified by using the equation 10 and 11.

3. Sound Pressure and Sound Pressure Level

Sound pressure is the pressure measured within the wave relative to the ambient air pressure. Quiet sounds produce sound waves with small sound pressures whereas loud sounds produce sound waves with large sound pressures. Sound pressure level is measured in decibels (dB) and can be calculated using the following equation, where p is the sound pressure of the sound wave and p_o is the reference sound pressure [21].

$$L_P = 20\, log_{10}\left(\frac{p}{p_0}\right) dB \qquad (13)$$

4. Results and discussion

The complete design for a unimorph MEMS piezoelectric cantilever array for fully cochlear implantable device with polysilicon-ZnO is simulated in COMSOL Multiphysics and the results are shown in figure 5 and figure 6. The proposed system consists of seventeen cantilevers in an array arrangement connected in parallel to produce the maximum electric potential voltage of

Annals of R.S.C.B., ISSN:1583-6258, Vol. 25, Issue 4, 2021, Pages. 618 - 639
Received 05 March 2021; Accepted 01 April 2021.

135mV at 300 Hz for a sound pressure level of 94dB. Pressure is applied as boundary load and the particular beam gets displacement on the z component. Figure 5 shows the displacement of $1.46 \times 10^{-3} \mu m$ to the corresponding beam at 1200 Hz. The device was simulated for 60 dB, 70 dB, 80 dB and 94 dB sound pressure level individually and the parameters such as von Mises stress(N/m^2), eigen frequency(Hz), displacement (µm), the electric potential voltage(mV/Pa) are obtained and shown in figure 6 and figure 7 .

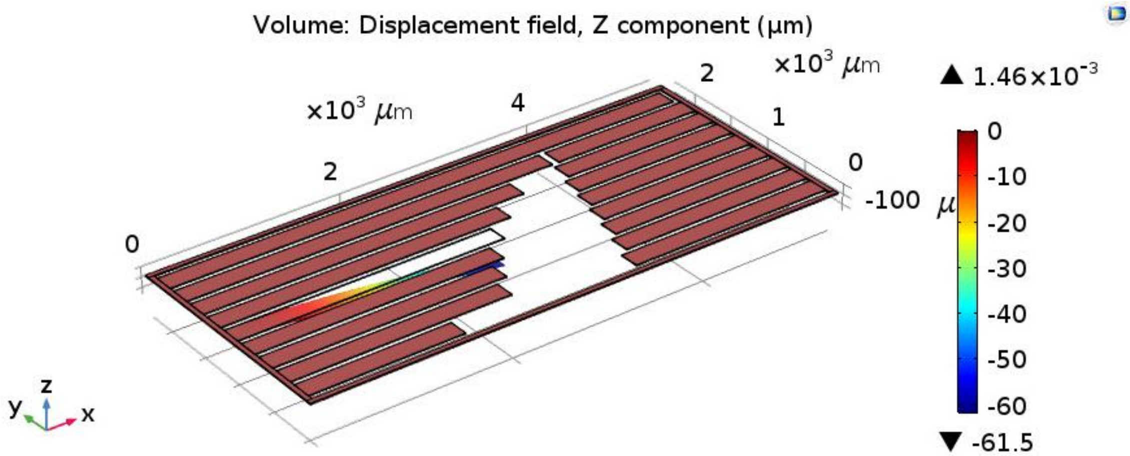

Figure 5. Tip displacement of the cantilever beam for 1200 Hz.

Annals of R.S.C.B., ISSN:1583-6258, Vol. 25, Issue 4, 2021, Pages. 618 - 639
Received 05 March 2021; Accepted 01 April 2021.

300 Hz

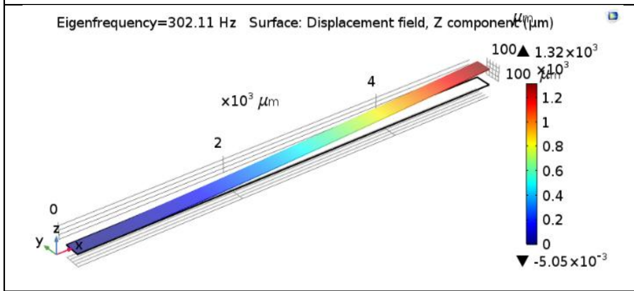

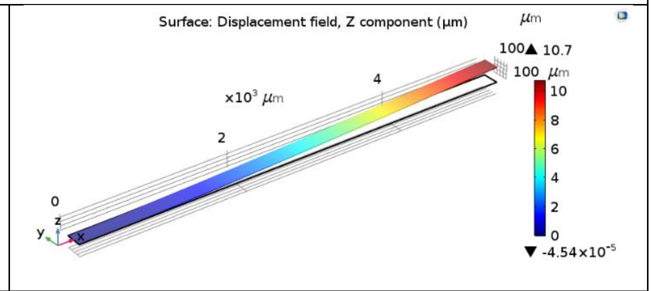

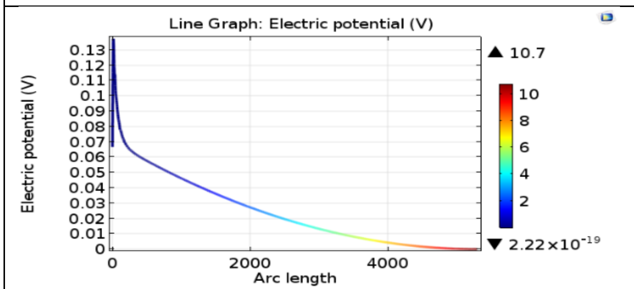

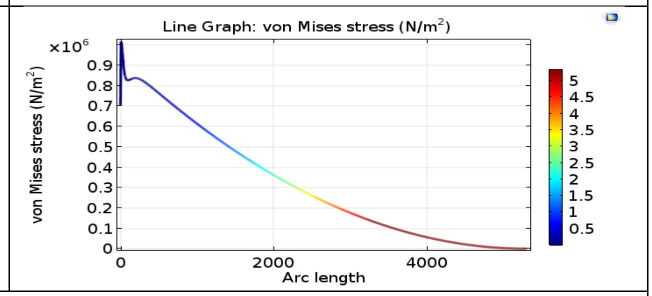

600 Hz

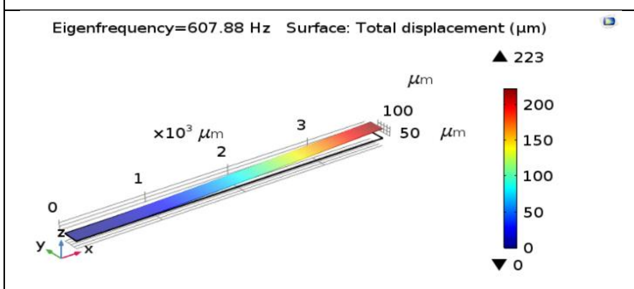

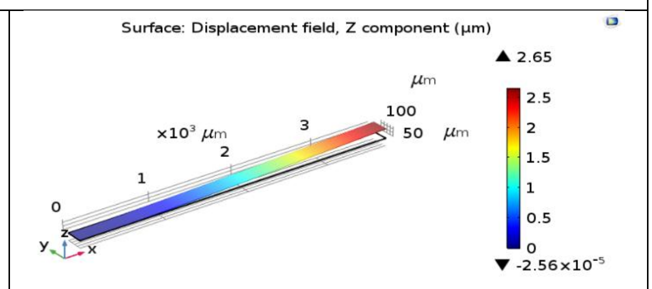

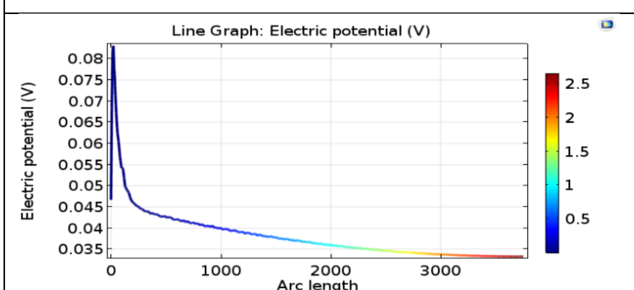

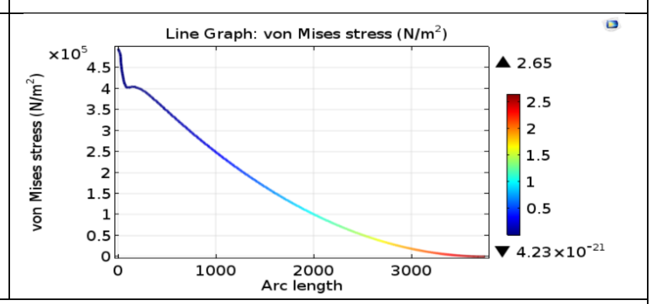

800 Hz

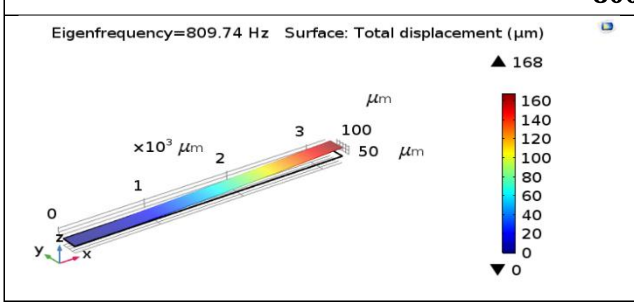

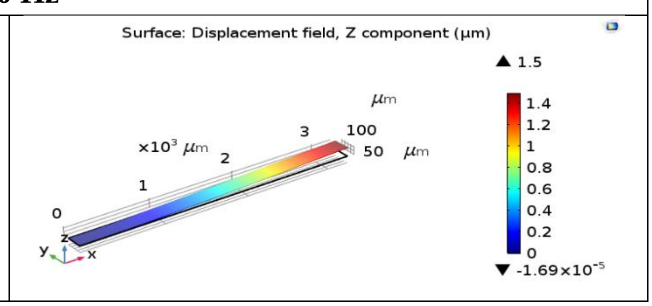

Annals of R.S.C.B., ISSN:1583-6258, Vol. 25, Issue 4, 2021, Pages. 618 - 639
Received 05 March 2021; Accepted 01 April 2021.

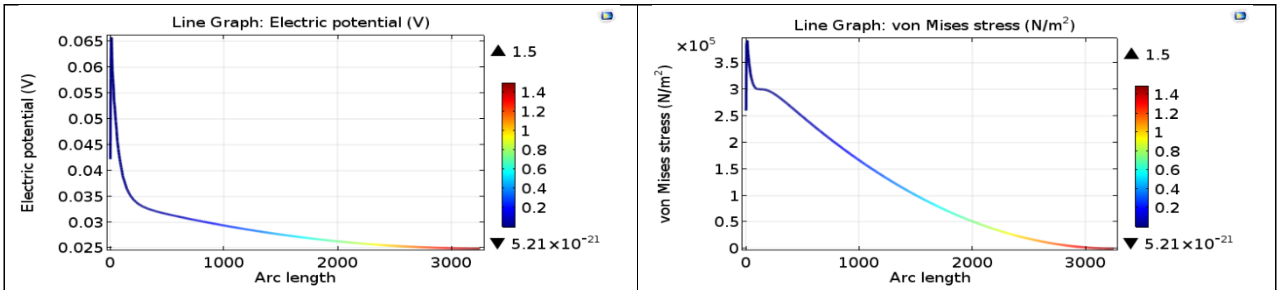

1000 Hz

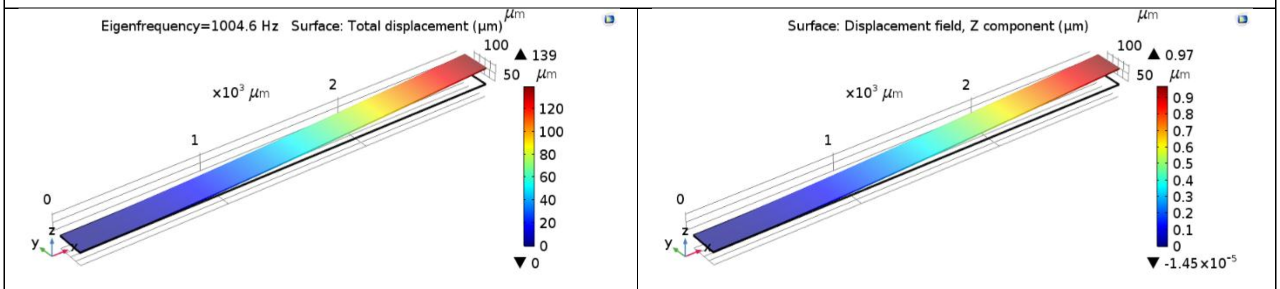

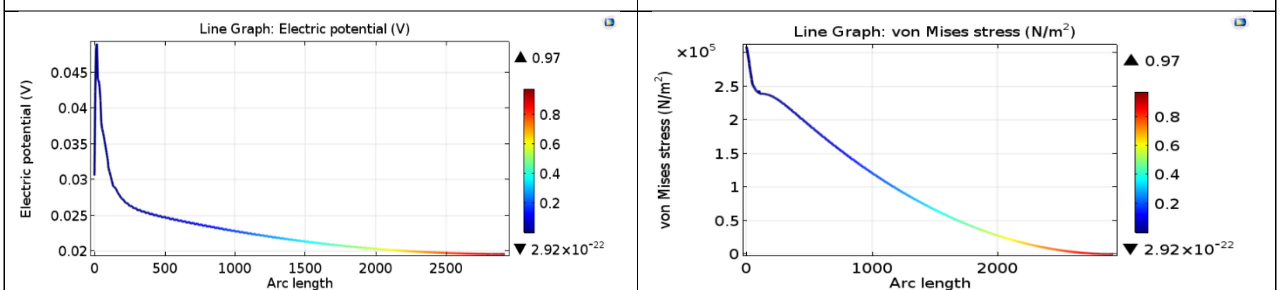

1200 Hz

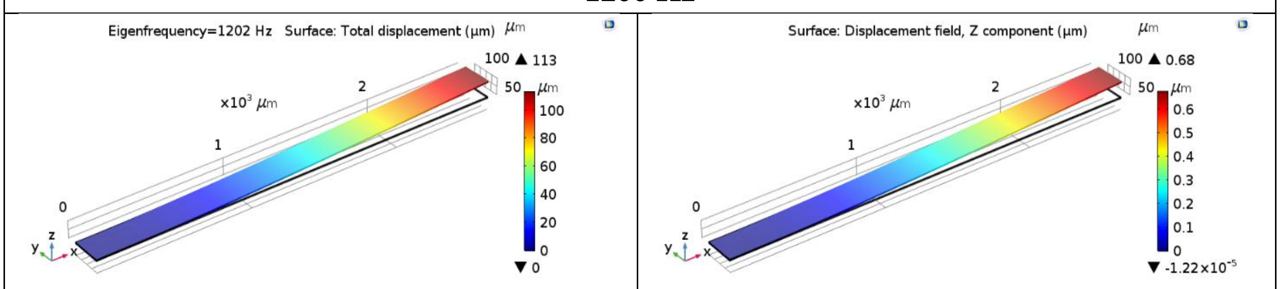

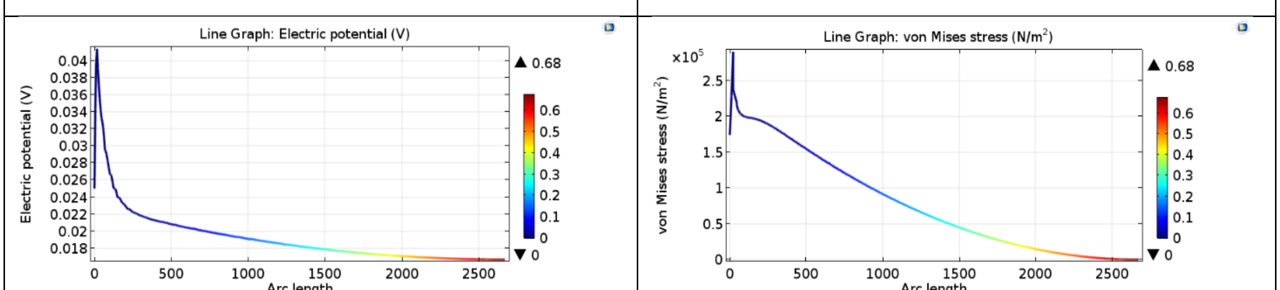

1400 Hz

Annals of R.S.C.B., ISSN:1583-6258, Vol. 25, Issue 4, 2021, Pages. 618 - 639
Received 05 March 2021; Accepted 01 April 2021.

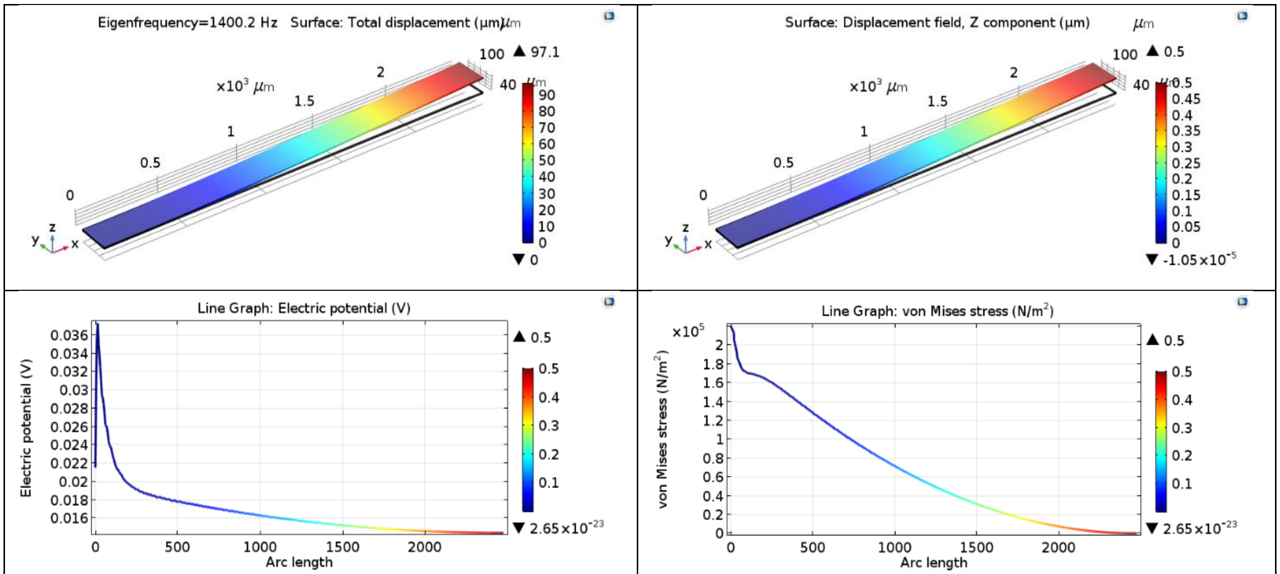

1600 Hz

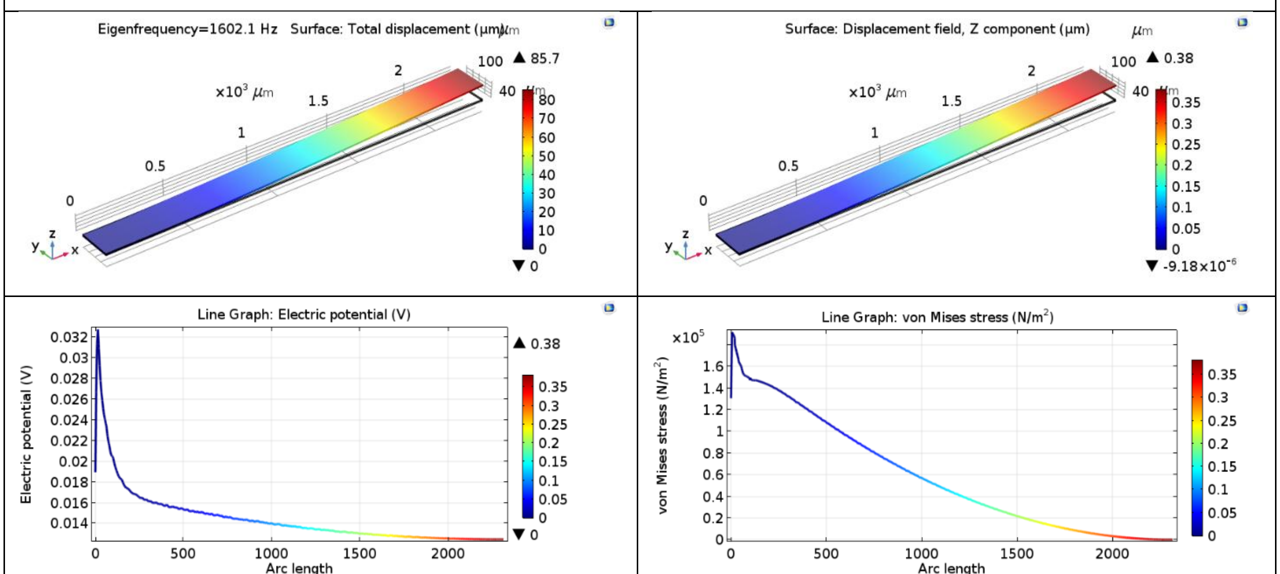

1800 Hz

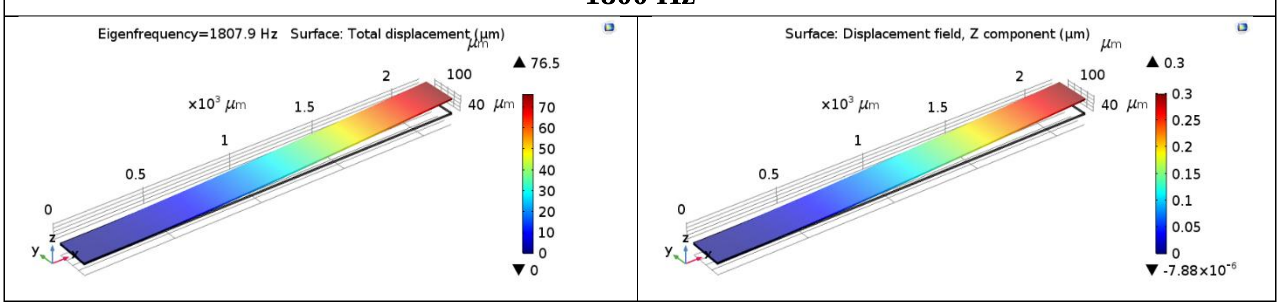

Annals of R.S.C.B., ISSN:1583-6258, Vol. 25, Issue 4, 2021, Pages. 618 - 639
Received 05 March 2021; Accepted 01 April 2021.

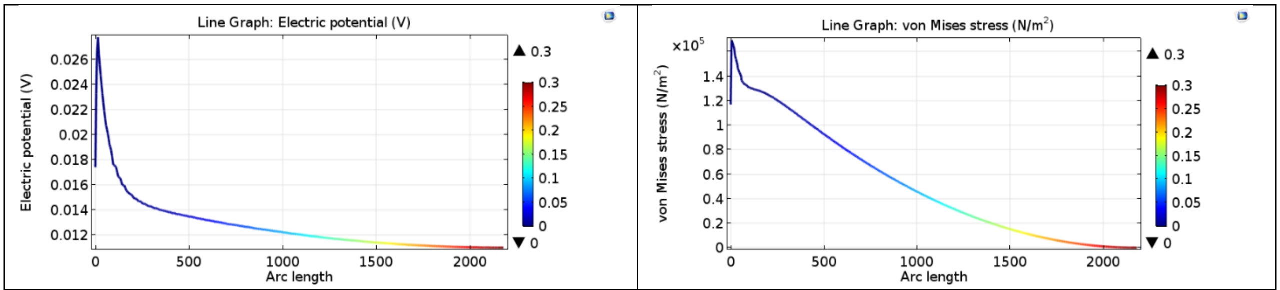

2000 Hz

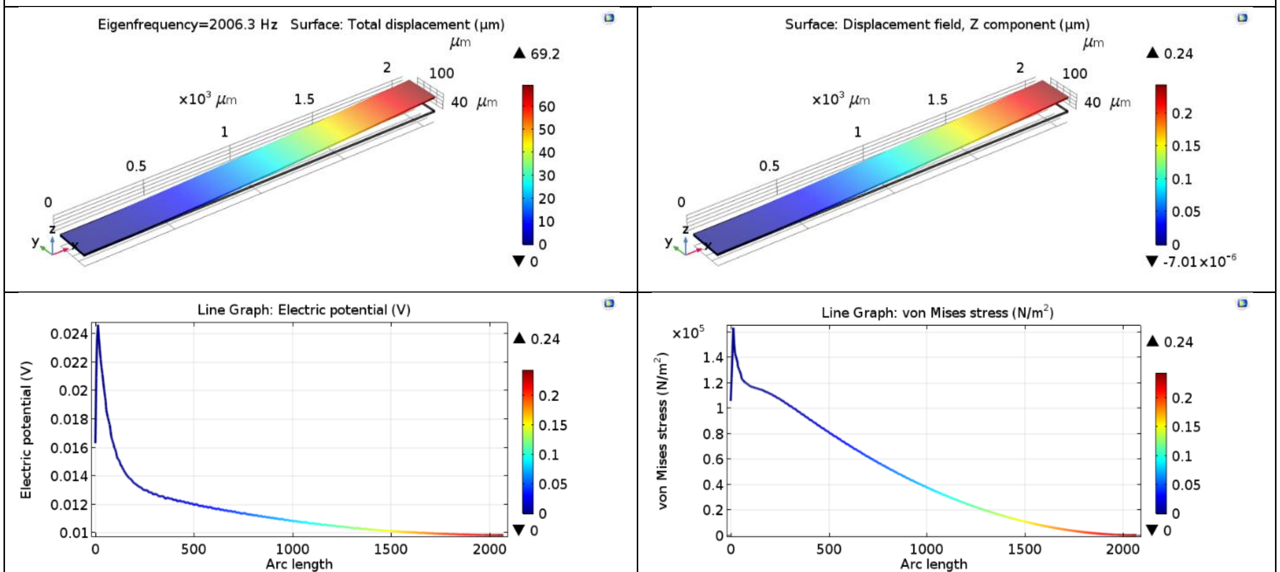

2200 Hz

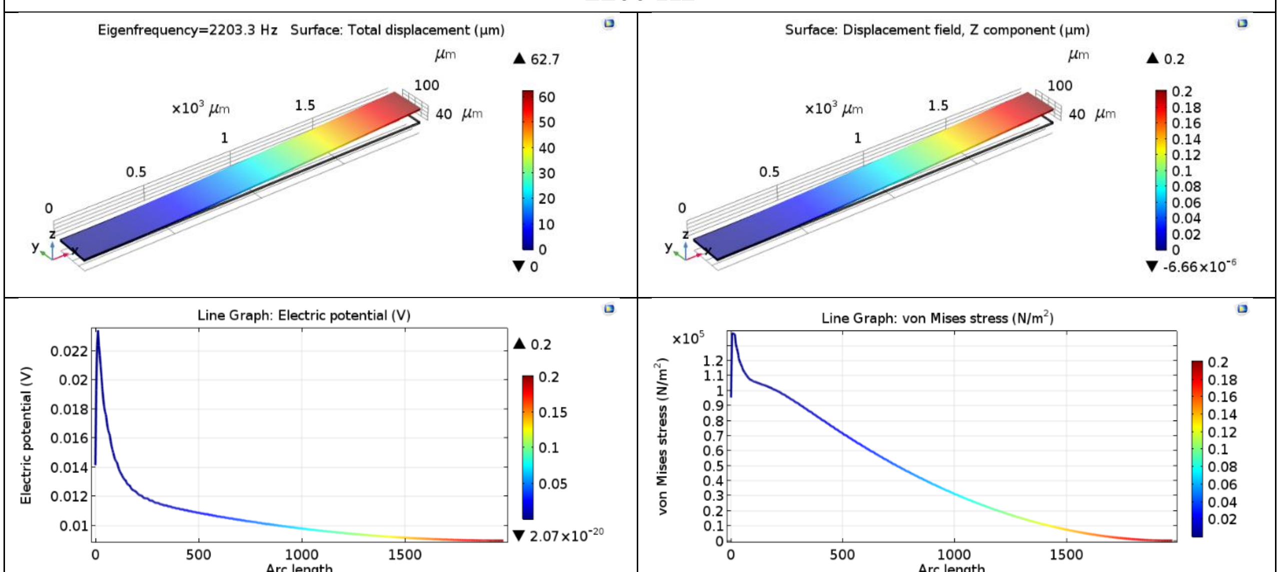

2400 Hz

Annals of R.S.C.B., ISSN:1583-6258, Vol. 25, Issue 4, 2021, Pages. 618 - 639
Received 05 March 2021; Accepted 01 April 2021.

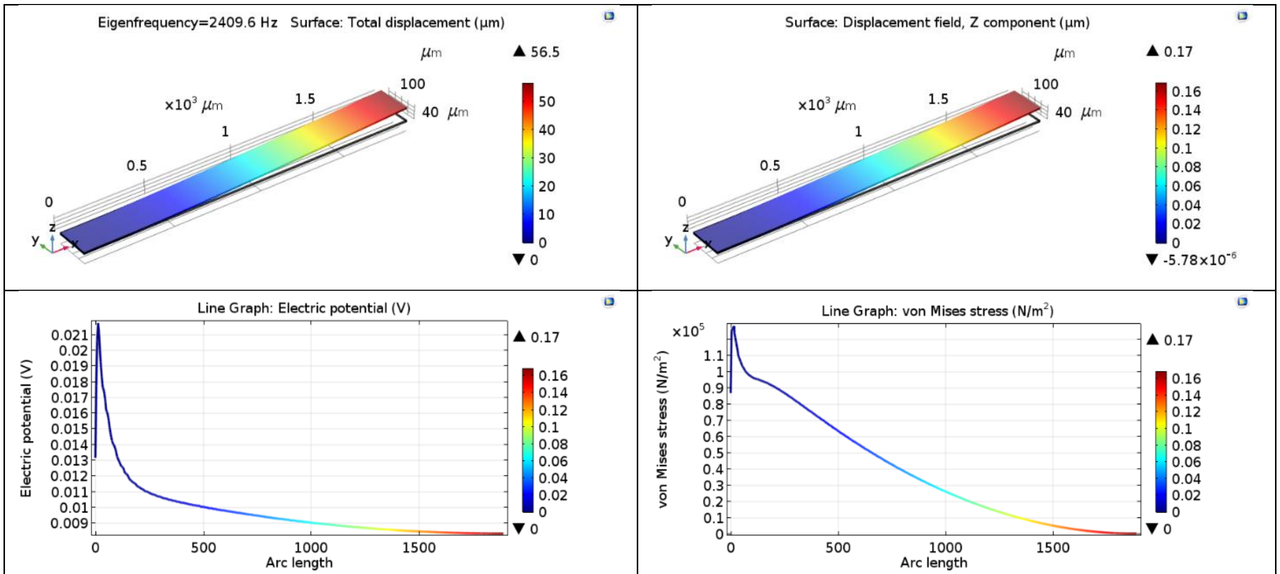

2600 Hz

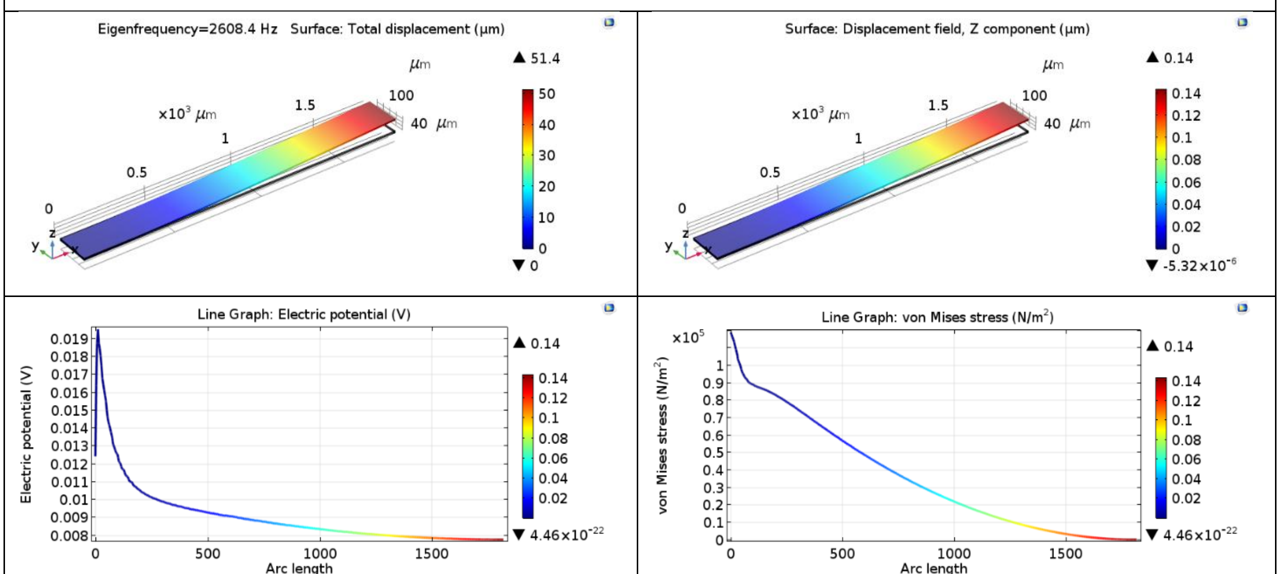

2800 Hz

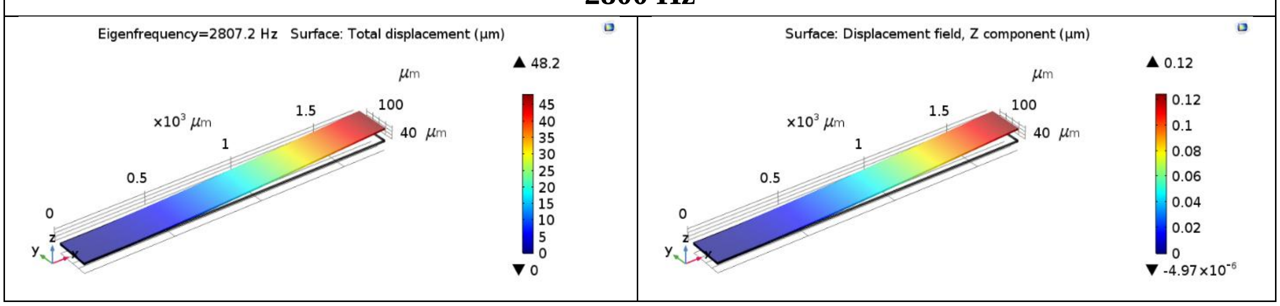

Annals of R.S.C.B., ISSN:1583-6258, Vol. 25, Issue 4, 2021, Pages. 618 - 639
Received 05 March 2021; Accepted 01 April 2021.

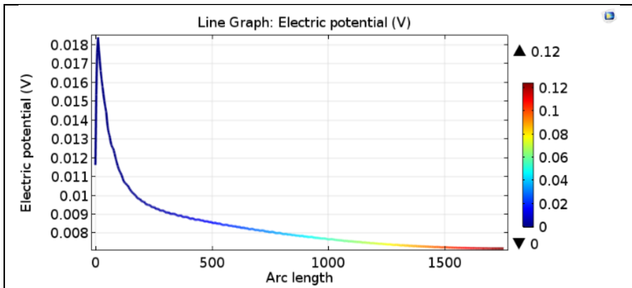

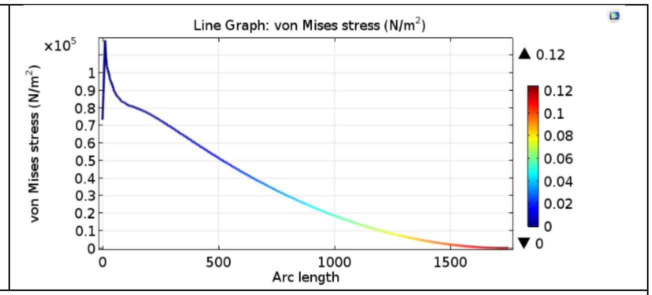

3000 Hz

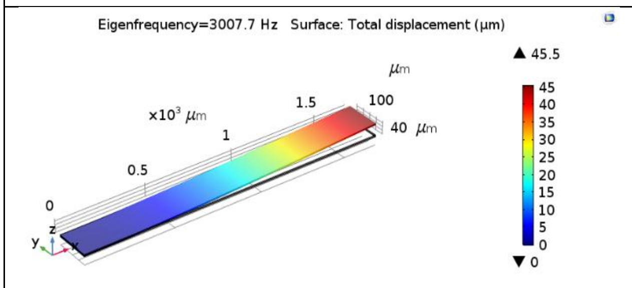

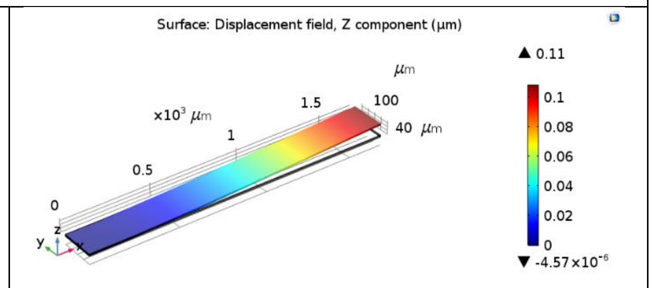

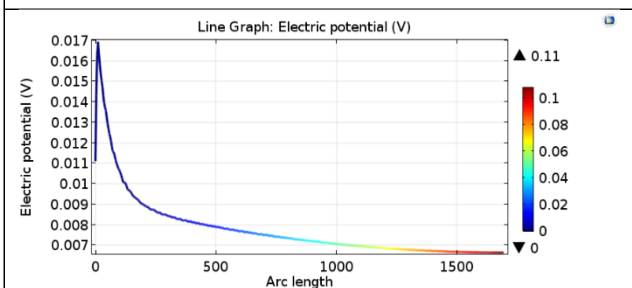

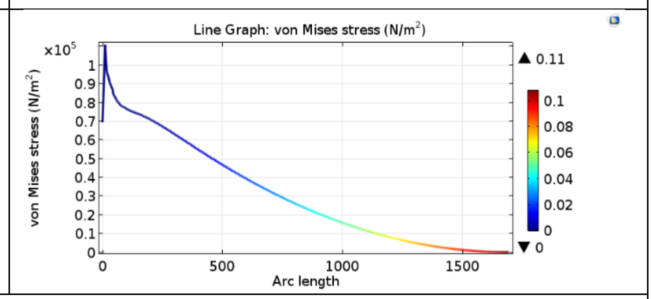

3300 Hz

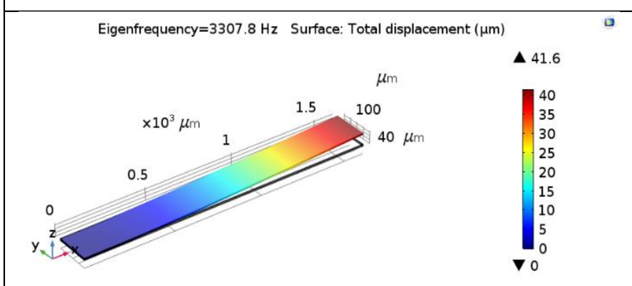

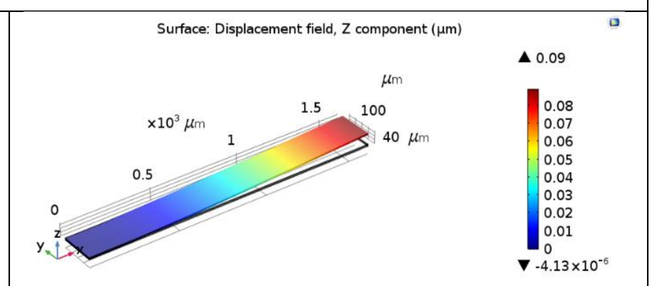

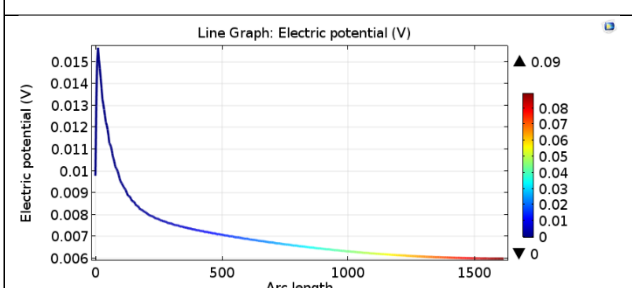

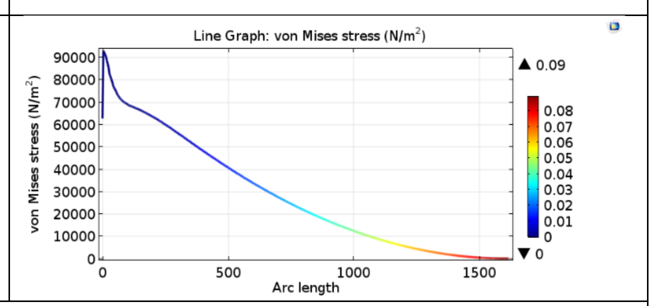

3500 Hz

Annals of R.S.C.B., ISSN:1583-6258, Vol. 25, Issue 4, 2021, Pages. 618 - 639
Received 05 March 2021; Accepted 01 April 2021.

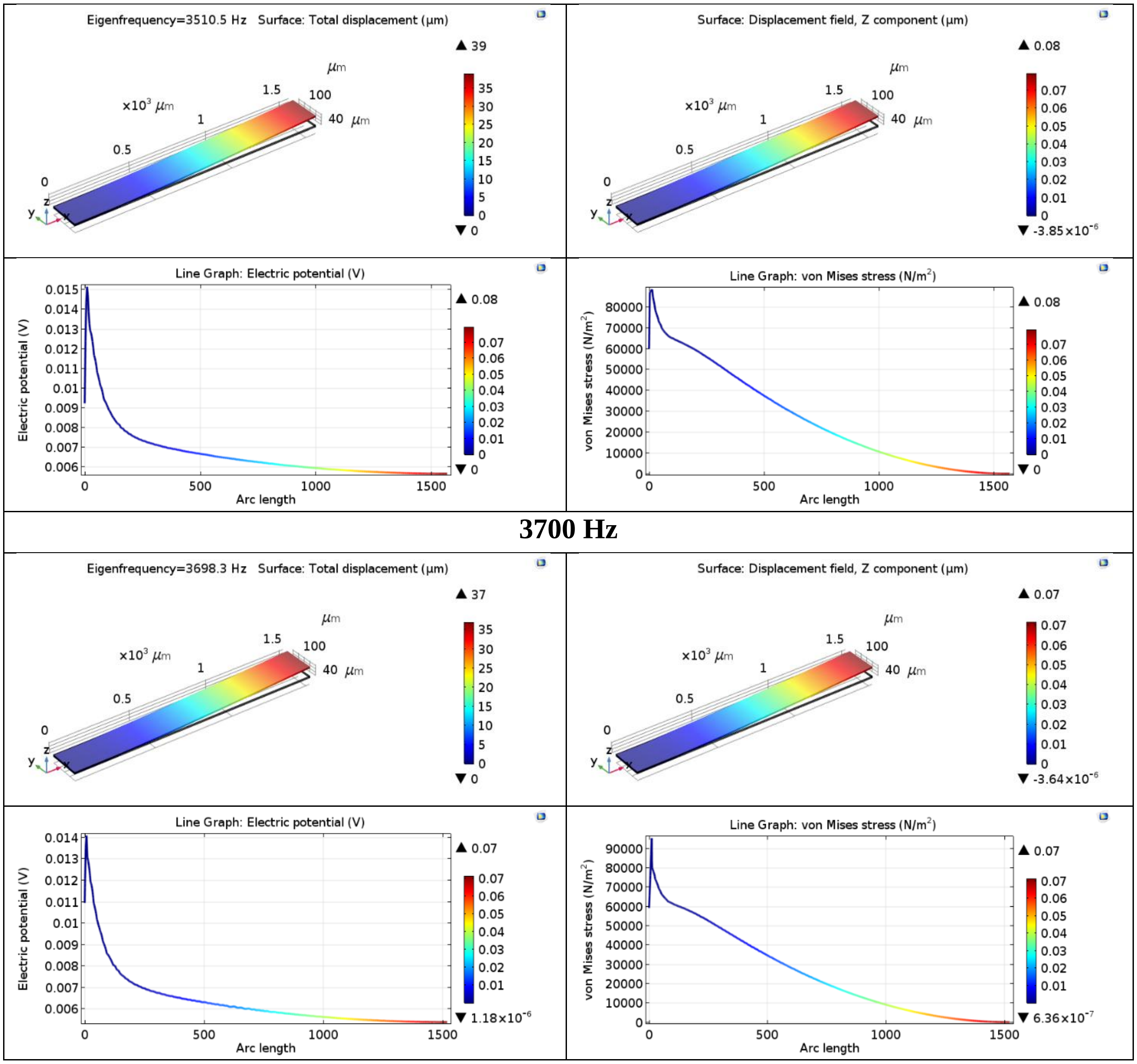

Figure 6. Eigen Frequency and Displacement profiles, Electric potential and von Mises stress plots for complete design module

Annals of R.S.C.B., ISSN:1583-6258, Vol. 25, Issue 4, 2021, Pages. 618 - 639
Received 05 March 2021; Accepted 01 April 2021.

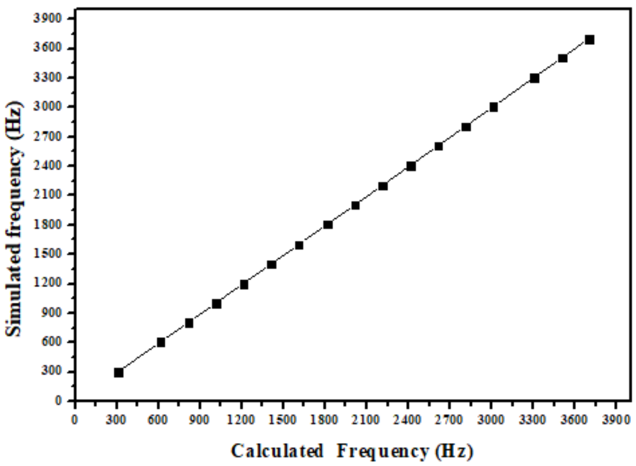

(a)

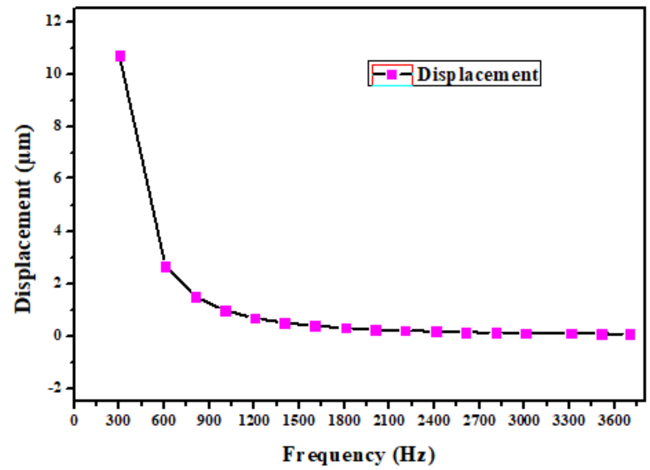

(b)

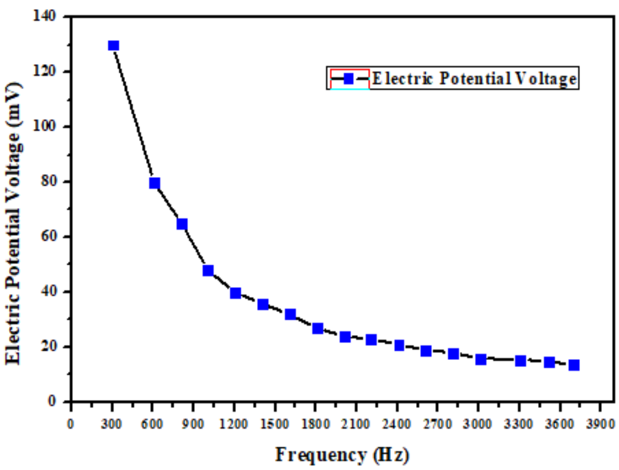

(c)

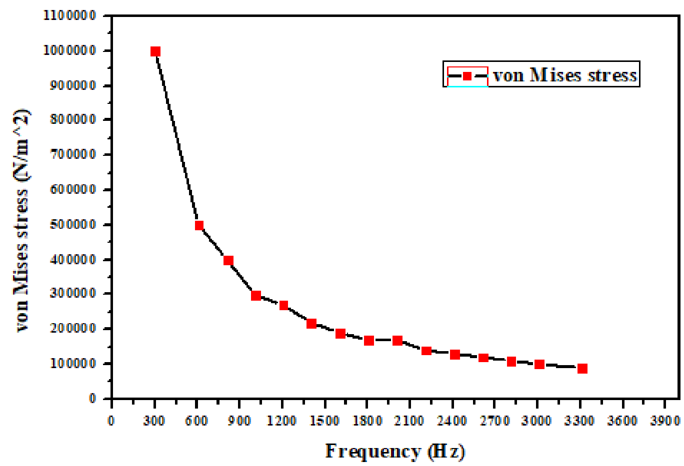

(d)

Annals of R.S.C.B., ISSN:1583-6258, Vol. 25, Issue 4, 2021, Pages. 618 - 639
Received 05 March 2021; Accepted 01 April 2021.

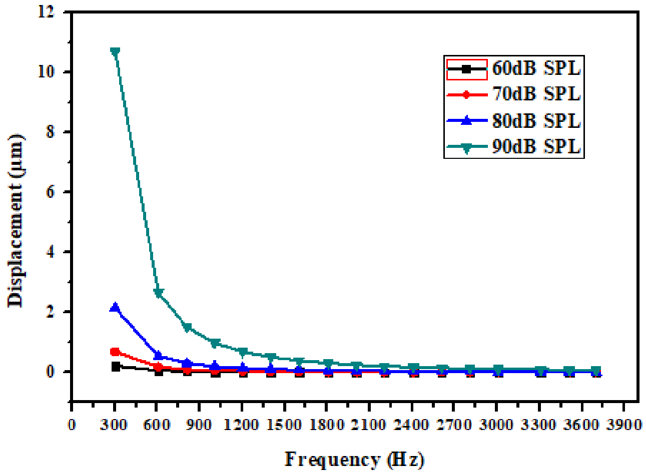

(e)

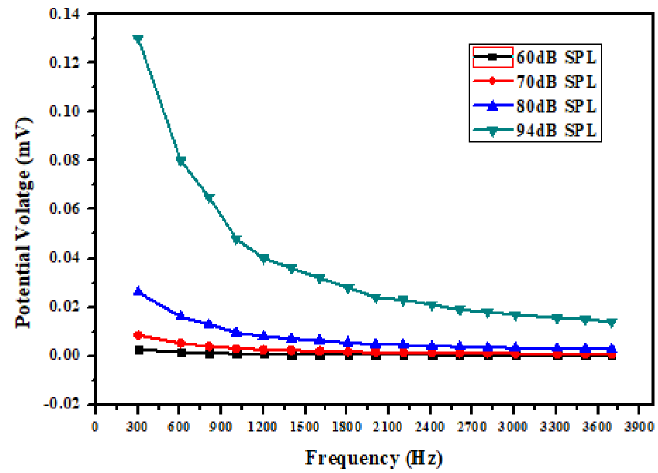

(f)

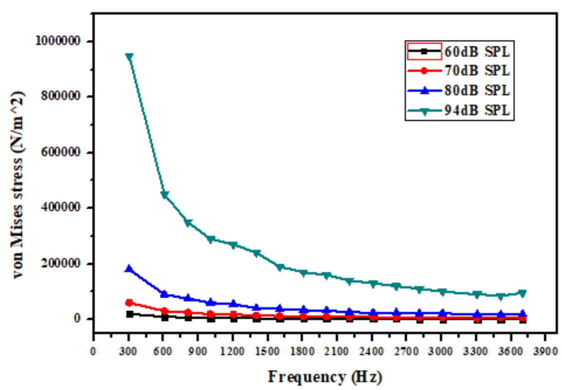

(g)

Figure 7. a) - Calculated frequency versus simulated frequency for complete design
b), c), d) - Displacement, induced electric potential voltage, Von Mises stress versus frequency plots simulated by COMSOL Multiphysics
e), f), g) - Displacement, Electric potential voltage, von Mises stress versus frequency for different inputs ranging from 60 to 94 dB SPL

Fig 7 a shows a linear curve which means the simulated frequency matches with the frequency calculated using equation 11. From Figure 7 b it is noted that displacement decreases exponentially with increase in frequency for an input of 94 dB SPL. Similarly, electric potential voltage and Von Mises Stress decreases with increase in frequency in the range of 300 to 3700 Hz and the corresponding curves are plotted in Figures 7 c and 7 d. Figures 7 e, f and g illustrates the displacement, Electric potential voltage, Von Mises stress versus frequency plots obtained for different input levels ranging from 60 to 94 dB. It can be observed that the parameters under study increase with the input sound pressure level.

Table 3 shows the comparison of existing MEMS piezoelectric acoustic sensors with the proposed sensor.

Table 3: Comparison of previous and current research findings.

Study	Cochlear Implant Applications	Number of cantilever Beams	Frequency range	Excitation	Maximum output voltage	Area
I	Thin Film PZT Acoustic Sensor	Eight cantilevers	300-4800 Hz	0.6g	24.79 mV @900 Hz	5 mm × 5mm
II	Spiral-Shaped Piezoelectric MEMS Cantilever Array	Sixteen cantilevers	300–700 Hz	1g	3–10 mV	2 mm × 2 mm
III	Thin film piezoelectric acoustic transducer	Eight cantilevers	250–5000 Hz	110 dB	114 mV	5 mm × 5 mm
IV	Multi-channel thin film piezoelectric acoustic transducer	Eight cantilever beam	316-5767 Hz	110dB	139.36 mV @316 Hz	5 mm ×5 mm
V	**This work**	**Seventeen cantilever beams**	**300-3700 Hz**	**60-94dB**	**138.6 mV @300 Hz**	**4.3 mm × 2.4 mm**

The Thin film PZT acoustic sensor proposed by İliket al. was fabricated with eight cantilevers. An SPL of 100dB is applied over the frequency range of 300-4800 Hz and the output voltage of 22.98mV was generated using a test setup of shaker-table [22].Udvardiet al.'s Spiral-Shaped Piezoelectric MEMS Cantilever Array was fabricated by bulk micromachining technique on a Si-on-Insulator (SOI) wafer and aluminum nitride (AlN) with sixteen cantilevers. A low frequency range of 300-700 Hz with an SPL of 110dB is applied, and a 9.6 mV output voltage was produced. To obtain this, an experiment was conducted on a 3D printed sample which was mounted on a shaker table [23]. Another Thin film piezoelectric acoustic transducer proposed by İliket al. has eight cantilevers. It produced 114mV for a frequency range of 250–5000 Hz and an input SPL of 110 dB. The characteristics of the sensor were obtained using Lase Doppler Vibrometer and the output voltage was measured using an Oscilloscope [24]. Yüksel et al. experimented with a Multi-channel thin film piezoelectric acoustic transducer which was fabricated with PLD-PZT piezoelectric layers, containing eight cantilever beams. An output voltage of 139.36 mV at 316.4 Hz under 110dB was obtained by Finite Element Method modeling for cantilever resonance frequencies and shaker-table experiments [25]. When compared to previous researches on MEMS piezoelectric acoustic transducers the device proposed in this work stands high as it accommodates seventeen cantilever beams within 4.3 x 2.6 mm, thus making it area efficient. It is capable of producing 138.6 mV at 94 dB SPL over the frequency range of 300-3700 Hz.

5. Conclusion

In this work, the proposed MEMS piezoelectric cantilever array (PCA) for a fully cochlear implantable sensor for stimulating the auditory nerve via cochlea was designed. The maximum electric potential voltage of 138.6 mV for a frequency of 300 Hz is generated at 94 dB SPL which makes it feasible and efficient by using unimorph cantilever beams. The drawbacks of conventional CI's are discomfort, damage of components, and battery replacement. The proposed method excludes these drawbacks by the use of a MEMS piezoelectric cantilever array as it generates potential voltage directly from the deflection of the device, which is placed in the eardrum. The main advantages of this device are reduced size, power consumption, cost, and maximum electric potential voltage. This system is viable for next-generation MEMS piezoelectric cantilever array implantable sensor for all applications as its performance is found to be better when compared to the existing MEMS piezoelectric acoustic sensors as shown in Table 3. In the future, the design can be improved and optimized to get maximum electric potential voltage, bandwidth, and quality factor.

ACKNOWLEDGEMENT

J. Abdul Aziz Khan received the B.E. degree in Electronics and Communication Engineering in 2011 and the M.E degree in Embedded System Technologies in 2015 Affiliated to Anna University, Chennai. He is presently pursuing his Ph.D in Microelectronics and MEMS, Annamalai University, Chidambaram. His area of research are MEMS Piezoelectric Sensors and Embedded Systems. He is a life member of the Indian Society for Technical Education.

P. Shanmugaraja was born in 1971 in Tirunelveli. He has obtained B.E (Electronics and Communication) from National Engineering College and M.E. (Medical Electronics) from Anna University Chennai, in 1992 and 1995 respectively and then Ph.D. in Micro Electronics from Annamalai university, Chidambaram in 2015. He is presently a Professor in Electronics and Instrumentation Engineering Department at Annamalai University where he has put in 24 years of service. He is presently guiding six Ph.D. scholars and has guided twenty-seven M.E students. His areas of interest are: Nano electronics, Embedded system, Medical electronics. He is a life member of Indian Society for Technical Education and annual Member in Instrumentation Systems and Automation

S. Kannan obtained a Bachelor's degree in Electronics and Communication Engineering at P.S.N.A College of Engineering, India in 2009. He obtained a Master's degree in Communication Systems from PRIST University, India in 2011. He later joined and worked 5 years as an Assistant professor in the department of Electronics and Communication Engineering in Chendhuran college of Engineering and Technology, India. He is currently pursuing his Ph.D in Microelectronics and MEMS at National MEMS Design Center, Annamalai University, India. His research interests include MEMS sensors and microfabrication.

REFERENCES

1. https://www.who.int/news-room/fact-sheets/detail/deafness-and-hearing-loss[2 March 2021].
2. Hunter, Lisa L., Brian B. Monson, David R. Moore, Sumitrajit Dhar, Beverly A. Wright, Kevin J. Munro, Lina Motlagh Zadeh, Chelsea M. Blankenship, Samantha M. Stiepan, and Jonathan H. Siegel. "Extended high frequency hearing and speech perception implications in adults and children." *Hearing research* (2020): 107922.
3. Monson, Brian B., and Jacob Caravello. "The maximum audible low-pass cutoff frequency for speech." *The Journal of the Acoustical Society of America* 146, no. 6 (2019): EL496-EL501.
4. Michels, Thomas C., Maribeth T. Duffy, and Derek J. Rogers. "Hearing loss in adults: differential diagnosis and treatment." *American family physician* 100, no. 2 (2019): 98-108.
5. Chandrasekhar, Sujana S., Betty S. Tsai Do, Seth R. Schwartz, Laura J. Bontempo, Erynne A. Faucett, Sandra A. Finestone, Deena B. Hollingsworth et al. "Clinical practice guideline: sudden hearing loss (update)." *Otolaryngology–Head and Neck Surgery* 161, no. 1_suppl (2019): S1-S45.
6. Weiss, Roxanne, Andreas Loth, Martin Leinung, Sven Balster, Daniel Hirth, Timo Stöver, Silke Helbig, and Sabine Kramer. "A new adhesive bone conduction hearing system as a treatment option for transient hearing loss after middle ear surgery." *European Archives of Oto-rhino-laryngology* 277, no. 3 (2020): 751-759.
7. Ontario, Health Quality. "Implantable Devices for Single-Sided Deafness and Conductive or Mixed Hearing Loss: A Health Technology Assessment." *Ontario health technology assessment series* 20, no. 1 (2020): 1.
8. Frear, Darcy L., Xiying Guan, Christof Stieger, John J. Rosowski, and Hideko Heidi Nakajima. "Impedances of the inner and middle ear estimated from intracochlear sound pressures in normal human temporal bones." *Hearing research* 367 (2018): 17-31.
9. Keidser, Gitte, and Elizabeth Convery. "Outcomes with a self-fitting hearing aid." *Trends in hearing* 22 (2018): 2331216518768958.
10. Zhu, Dawei, Xuefeng Shi, Stephen Nicholas, Xin Ye, Siyuan Chen, and Ping He. "Preferences for hearing aid attributes among people with moderate or greater hearing loss in rural China: A discrete choice experiment." *Patient preference and adherence* 14 (2020): 643.
11. Johnstone, Patti M., Kristen ET Mills, Elizabeth Humphrey, Kelly R. Yeager, Emily Jones, Kelly McElligott, Amy Pierce, Smita Agrawal, Crista Froeling, and John P. Little. "Using microphone technology to improve speech perception in noise in children with cochlear implants." *J Am Acad Audiol* 29, no. 09 (2018): 814-825.
12. Lee, Youngmee, and Hyunsub Sim. "Bilateral cochlear implantation versus unilateral cochlear implantation in deaf children: Effects of sentence context and listening

conditions on recognition of spoken words in sentences." *International Journal of Pediatric Otorhinolaryngology* 137 (2020): 110237.

13. Sachse, M., W. Hortschitz, M. Stifter, H. Steiner, and T. Sauter. "Design of an implantable seismic sensor placed on the ossicular chain." *Medical engineering & physics* 35, no. 10 (2013): 1399-1405.

14. Yip, Marcus, Rui Jin, Hideko Heidi Nakajima, Konstantina M. Stankovic, and Anantha P. Chandrakasan. "A fully-implantable cochlear implant SoC with piezoelectric middle-ear sensor and arbitrary waveform neural stimulation." *IEEE journal of solid-state circuits* 50, no. 1 (2014): 214-229.

15. Yüksel, Muhammed Berat, Bedirhan İlik, Aziz Koyuncuoğlu, and Haluk Külah. "Multi-channel thin film piezoelectric acoustic transducer for cochlear implant applications." In *2019 IEEE SENSORS*, pp. 1-4. IEEE, 2019.

16. Ghoddus, Hossein, and Zoheir Kordrostami. "Harvesting the ultimate electrical power from mems piezoelectric vibration energy harvesters: an optimization approach." *IEEE Sensors Journal* 18, no. 21 (2018): 8667-8675.

17. Han, Jae Hyun, Jun-Hyuk Kwak, Daniel Juhyung Joe, Seong Kwang Hong, Hee Seung Wang, Jung Hwan Park, Shin Hur, and Keon Jae Lee. "Basilar membrane-inspired self-powered acoustic sensor enabled by highly sensitive multi tunable frequency band." *Nano Energy* 53 (2018): 198-205.

18. Gesing, A. L., F. D. P. Alves, S. Paul, and J. A. Cordioli. "On the design of a MEMS piezoelectric accelerometer coupled to the middle ear as an implantable sensor for hearing devices." *Scientific reports* 8, no. 1 (2018): 1-10.

19. Wang, Peihong, and Hejun Du. "ZnO thin film piezoelectric MEMS vibration energy harvesters with two piezoelectric elements for higher output performance." *Review of Scientific Instruments* 86, no. 7 (2015): 075002.

20. Raaja, Bhaskaran Prathish, Rathnam Joseph Daniel, and Koilmani Sumangala. "A simple analytical model for MEMS cantilever beam piezoelectric accelerometer and high sensitivity design for SHM (structural health monitoring) applications." *Transactions on Electrical and Electronic Materials* 18, no. 2 (2017): 78-88.

21. Tseng, Shih-Hsiung, Sung-Cheng Lo, Yi-Jia Wang, Shih-Wei Lin, Mingching Wu, and Weileun Fang. "Sound Pressure and Low Frequency Enhancement Using Novel PZT MEMS Microspeaker Design." In *2020 IEEE 33rd International Conference on Micro Electro Mechanical Systems (MEMS)*, pp. 546-549. IEEE, 2020.

22. İlik, Bedirhan, Aziz Koyuncuoğlu, Hasan Uluşan, Salar Chamanian, Dilek Işık, Özlem Şardan-Sukas, and Haluk Külah. "Thin film PZT acoustic sensor for fully implantable cochlear implants." In *Multidisciplinary Digital Publishing Institute Proceedings*, vol. 1, no. 4, p. 366. 2017.

23. Udvardi, Péter, János Radó, András Straszner, János Ferencz, Zoltán Hajnal, Saeedeh Soleimani, Michael Schneider, Ulrich Schmid, Péter Révész, and János Volk. "Spiral-

Annals of R.S.C.B., ISSN:1583-6258, Vol. 25, Issue 4, 2021, Pages. 618 - 639
Received 05 March 2021; Accepted 01 April 2021.

shaped piezoelectric MEMS cantilever array for fully implantable hearing systems." *Micromachines* 8, no. 10 (2017): 311.

24. Ilik, Bedirhan, Aziz Koyuncuoğlu, Özlem Şardan-Sukas, and Haluk Külah. "Thin film piezoelectric acoustic transducer for fully implantable cochlear implants." *Sensors and Actuators A: Physical* 280 (2018): 38-46.

25. Yüksel, Muhammed Berat, Bedirhan İlik, Aziz Koyuncuoğlu, and Haluk Külah. "Multi-channel thin film piezoelectric acoustic transducer for cochlear implant applications." In *2019 IEEE SENSORS*, pp. 1-4. IEEE, 2019.